

"© 2016 IEEE. Personal use of this material is permitted. Permission from IEEE must be obtained for all other uses, in any current or future media, including reprinting/republishing this material for advertising or promotional purposes, creating new collective works, for resale or redistribution to servers or lists, or reuse of any copyrighted component of this work in other works."

# Effect of CSI Quantization on the Average Rate in MU-MIMO WLANs

Sanjeeb Shrestha\*, Gengfa Fang\*, Eryk Dutkiewicz\* and Xiaojing Huang†

\*Department of Engineering, Macquarie University, Sydney, Australia

†University of Technology, Sydney, Australia

Email: sanjeeb.shrestha@mq.edu.au

**Abstract**—In Multi-User Multiple Input Multiple Output (MU-MIMO) Wireless Local Area Networks (WLANs), the optimal-solution such as Dirty Paper Coding (DPC) or the sub-optimal solution Zeroforcing Beamforming (ZFB) with perfect Channel State Information (CSI), is practically limited due to the complexity and the non-availability of perfect CSI at the Access Points (APs)/transmitters. In such a context, ZFB based on channel quantization available at the APs (ZFQ) is the obvious choice for the Multi-User transmission strategy. However, since the quantized CSI is used instead of the perfect CSI at the APs, the quantization error and its impact on the average rate for ZFQ have to be quantified in MU-MIMO WLAN settings. In this paper, we derive a closed-form expression for the upper bound of the channel quantization error and the average rate reduction due to the quantization error with respect to the perfect CSI at the APs. In MU-MIMO WLAN settings, our analytical and numerical studies show that, with an increasing number of antennas at the clients, both the quantization error bound and the average rate reduction increase for ZFQ, in comparison to the ZFB with the perfect CSI.

**Index terms**— Zeroforcing Beamforming, Channel State Information, Quantization Error, Average Rate Reduction.

## I. INTRODUCTION

Multi-User Multiple Input Multiple Output (MU-MIMO) based Wireless Local Area Networks (WLANs) are considered to be one of the prominent candidates for providing seamless high-data-rate experiences to clients with heterogeneous antennas such as iPhones (single antenna), Laptops, HDTV etc., (multiple antennas). However, basic results on the capacity of MU channels show that the optimal-solution Dirty Paper Coding (DPC) [1] is complexity limited [2]. Thus, the sub-optimal solution based on linear precoding such as Zeroforcing Beamforming (ZFB) [3] has emerged as a pragmatic choice for a MU transmission strategy. However, ZFB in MU-MIMO in WLANs is challenging; first, owing to the constraints such as: channel estimation errors at the receivers/clients, limited bandwidth of the feedback path, delay in feedback path, cost of feedback overheads etc. Thus the way out may be to provide a partial CSI in a quantized form to the APs and analyze the impact of CSI quantization in the system. Second, unlike cellular systems, MU-MIMO WLANs possess heterogeneous antennas clients, meaning that mobile devices have a single antenna, whereas Laptops and HDTV etc., can have two or more antennas within WLAN settings. This specific condition may require the APs to first collect all the required channel

realizations at one instant before concurrent transmissions to the clients [4],[5].

In this paper, we consider a practical case with Limited Feedback/Finite Rate Feedback (FRF) in MU-MIMO WLANs. First, we analyze the quantization error bound incurred by the quantized CSI. Second, we analyze the average rate reduction considering the ZFB based on channel quantization available at the APs (ZFQ). We derive a closed form expression for the quantization error bound and show its implications in the average rate reduction in comparison to ZFB with perfect CSI.

FRF was studied in [6],[7],[8], and the effects of CSI quantization have been primarily studied in [9],[10] considering different scenarios. However, most work in FRF is modeled for a MISO system and is related to cellular systems. Few have considered MIMO settings and estimated error bound and capacity. Related studies in [11],[12] calculate the asymptotic capacity for beamforming and have shown that the Random Vector Quantization (RVQ) scheme is asymptotically optimal. Our work is partly motivated by the aforementioned work, however, as the scenario we have considered is different, the error bound derived earlier becomes invalid. Since we consider MU-MIMO WLANs, the total feedback bandwidth  $T_{fb}$  and feedback bits  $B$  are finite, whereas the number of antennas at the clients are heterogeneous. Thus, we study the quantization error bound and the average rate reduction with FRF in MU-MIMO WLANs.

Notation: The superscript  $(.)^H$  denotes the Hermitian transpose whereas the operators  $\mathbb{E}[\cdot]$  and  $\|\cdot\|$  denote the expectation and the Euclidean norm respectively.  $\beta(\cdot)$  and  $\Gamma(\cdot)$  represent the Beta and the Gamma functions. The matrices, vectors and scalars are defined next, as they are used.

The rest of the paper is organized as follows. Section II presents the system model whereas Section III deals with the expected quantization error for MU-MIMO WLANs. In Section IV rate reduction for ZFB with FRF is studied. Section V gives numerical analysis and a conclusion is presented in Section VI.

## II. SYSTEM MODEL

We consider a MU-MIMO WLAN with  $K$  APs and clients as shown in Fig.1a. The APs have  $N$  antennas and clients have heterogeneous antennas denoted by variable  $M$ . An enlarged form of the  $j$ th AP client pair with FRF is shown in Fig.1b.

We take as reference the  $j$ th network AP and client ‘Bob’ for our analysis.

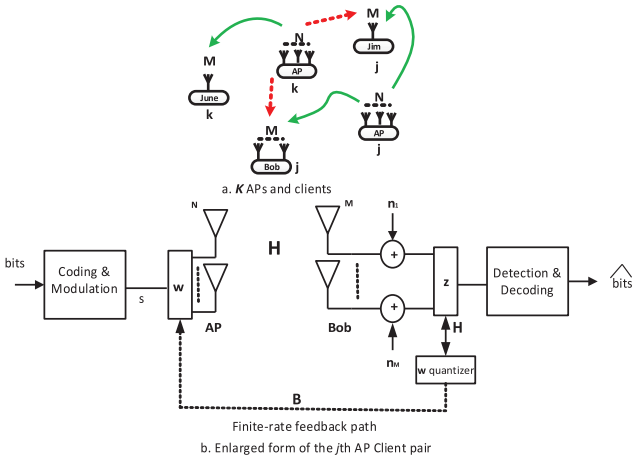


Fig. 1. System Model for Finite Rate Feedback.

The received signal  $y_j$  at the  $j$ th receiver/client ‘Bob’ is given by

$$y_j = \mathbf{z}_j^H \mathbf{H}_{jj}^H \mathbf{v}_j s_j + \sum_{i=1, i \neq j}^K \mathbf{z}_i^H \mathbf{H}_{ij}^H \mathbf{v}_i s_i + \mathbf{z}_j^H \mathbf{n}_j \quad (1)$$

where  $\mathbf{z} \in \mathbb{C}^{M \times 1}$  and  $\mathbf{v} \in \mathbb{C}^{N \times 1}$  are combining and beamforming vectors respectively. The channels  $\mathbf{H}_{jj} \in \mathbb{C}^{N \times M}$ ,  $\mathbf{H}_{ij} \in \mathbb{C}^{N \times M}$  are i.i.d. Rayleigh fading.  $\mathbf{n} \in \mathbb{C}^{M \times 1}$  represents noise at the client which is independent complex Gaussian random process with variance  $\sigma^2 = 1$ .  $s_j$  is the scalar complex symbol intended for the  $j$ th client. Symbol power is given by  $\mathbb{E}[|s|^2] = P$ .

We make the following assumptions. First, the feedback path has limited bandwidth  $T_{fb}$  which is error free, low rate and with zero delay. Second, the channel varies according to the block fading model where channels change independently from block to block. Third, the clients have the perfect CSI which allows us to neglect the channel estimation error.

Each client at the beginning of the block fading quantizes their channels to  $B$  bits and feeds back the quantization index instantaneously to the APs. The quantization is performed using a quantization codebook  $\mathcal{C}$  based on Random Vector Quantization (RVQ). The codebook is known to both the APs and the clients. We normalize the CSI as  $\tilde{\mathbf{H}}_{jj} \triangleq \frac{\mathbf{H}_{jj}}{\|\mathbf{H}_{jj}\|}$ . For channel quantization, each of the columns of the normalized channel matrix  $\tilde{\mathbf{H}}_{jj} = [\tilde{\mathbf{h}}_1, \tilde{\mathbf{h}}_2, \dots, \tilde{\mathbf{h}}_j, \dots, \tilde{\mathbf{h}}_M]$  where  $\tilde{\mathbf{h}}_j \in \mathbb{C}^{N \times 1}$  first individually quantizes with a codebook consisting of quantization vectors  $\mathcal{C} \triangleq \{\mathbf{w}_1, \mathbf{w}_2, \dots, \mathbf{w}_{2^B}\}$  that forms a minimum angle to it [7],[8]. Thus

$$\hat{\mathbf{h}}_j = \arg \min_{\mathbf{w} \in \mathcal{C}} \sin^2(\angle(\tilde{\mathbf{h}}_j, \mathbf{w})) \quad (2)$$

and  $\hat{\mathbf{H}} = [\hat{\mathbf{h}}_1, \hat{\mathbf{h}}_2, \dots, \hat{\mathbf{h}}_j, \dots, \hat{\mathbf{h}}_M]$ . The quantization error is given by

$$Z \triangleq \sin^2(\angle(\tilde{\mathbf{h}}_j, \hat{\mathbf{h}}_j)). \quad (3)$$

It is to be noted that the increase in the number of antennas at the clients,  $M$ , effectively increases the quantization codebook size from  $2^B$  to  $M \cdot 2^B$ .

Let  $I_j^F$  be the set of indices of clients. Then  $I_j^F = \{1 \leq j \leq U\}$  is the feedback index of the  $j$ th client out of  $U$  clients who feedback to the  $j$ th AP, i.e.,  $I_j^F \in I_U^F$ . The Channel Quality Indicator (CQI) is not included in the  $T_{fb}$ , and is perfectly known to the APs.

### III. EXPECTED QUANTIZATION ERROR FOR MU-MIMO WLANS

In MU-MIMO WLAN settings, the number of antenna at APs,  $N$ , is fixed whereas the number of antennas at clients,  $M$ , is variable. We take feedback bits  $B$  as an offline design parameter, meaning that per-user feedback bits are decided beforehand for a given fixed feedback bandwidth  $T_{fb}$ . In such a context, when  $M = 1$  then all  $B$  bits are used to quantize the channel vector of size  $N \times 1$ . However, when  $M > 1$  the rank of channel matrix  $\mathbf{H}$  is increased with increasing i.i.d. columns. Hence, assuming an isotropic distribution of  $B$ , the number of feedback bits per column is given by  $\lambda = \frac{B}{M}$ . The complementary cumulative distribution of the quantization error  $Z$  [13] is given by

$$\Pr(\sin^2(\angle(\tilde{\mathbf{h}}_j, \hat{\mathbf{h}}_j)) \geq z) = (1 - z^{N-1})^{2^{(\lambda)}}. \quad (4)$$

Thus we can write

$$\mathbb{E}[\sin^2(\angle(\tilde{\mathbf{h}}_j, \hat{\mathbf{h}}_j))] = \int_0^1 (1 - z^{N-1})^{2^{(\lambda)}} dz. \quad (5)$$

The Integral representation of the Beta function [14, p.5] gives

$$\beta\left(c, \frac{a}{b}\right) = b \int_0^1 z^{a-1} (1 - z^b)^{c-1} dz, \quad a > 0, b > 0, c > 0. \quad (6)$$

Substituting  $a = 1$ ,  $b = N - 1$  and  $c = (2^{(\lambda)} + 1)$  we get

$$\beta\left(2^{(\lambda)} + 1, \frac{1}{N-1}\right) = N - 1 \int_0^1 z^{1-1} (1 - z^{N-1})^{2^{(\lambda)}} dz. \quad (7)$$

From (5) and (7) we get

$$\begin{aligned} \mathbb{E}[\sin^2(\angle(\tilde{\mathbf{h}}_j, \hat{\mathbf{h}}_j))] &= \frac{1}{N-1} \beta\left(2^{(\lambda)} + 1, \frac{1}{N-1}\right) \\ &= \frac{2^{(\lambda)} \Gamma(2^{(\lambda)}) \Gamma(1 + \frac{1}{N-1})}{\Gamma(2^{(\lambda)} + 1 + \frac{1}{N-1})}. \end{aligned} \quad (8)$$

For the analytical expression (8) we have used the property  $\Gamma(x+1) = x\Gamma(x)$ . Now, calculating for  $N > 2$  we get

$$\begin{aligned} \mathbb{E}[\sin^2(\angle(\tilde{\mathbf{h}}_j, \hat{\mathbf{h}}_j))] &\leq \frac{2^{(\lambda)} \Gamma(2^{(\lambda)})}{\Gamma(2^{(\lambda)} + 1 + \frac{1}{N-1})} \\ &= \frac{\Gamma(2^{(\lambda)} + 1)}{\Gamma(2^{(\lambda)} + 1 + \frac{1}{N-1})}. \end{aligned} \quad (9)$$

The inequality follows from the convexity of the gamma function [15]  $\Gamma(x) \leq 1$  for  $1 \leq x \leq 2$  and the fact that

$\Gamma(1) = \Gamma(2) = 1$ . Now by applying Kershaw's inequality for the gamma function [16] we have

$$\frac{\Gamma(x+s)}{\Gamma(x+1)} < \left(x + \frac{s}{2}\right)^{s-1}, \quad \forall x > 0, 0 < s < 1. \quad (10)$$

Substituting  $x = (2^{\lambda} + \frac{1}{N-1})$  and  $s = (1 - \frac{1}{N-1})$  in (10) we can write (9) as

$$\begin{aligned} & \mathbb{E} \left[ \sin^2(\angle(\tilde{\mathbf{h}}_j, \hat{\mathbf{h}}_j)) \right] \\ & < \left( 2^{\lambda} + \frac{1}{N-1} + \frac{1}{2} \left( 1 - \frac{1}{N-1} \right) \right)^{-\frac{1}{N-1}} \\ & < \left( 2^{\lambda} + \frac{N}{2(N-1)} \right)^{-\frac{1}{N-1}}. \end{aligned} \quad (11)$$

In (11), for  $N = 2$ , the term  $(\frac{N}{2(N-1)}) = 1$  and for  $N > 2$ ,  $(\frac{N}{2(N-1)}) < 1$ , thus we can approximately rewrite (11) as

$$\mathbb{E} \left[ \sin^2(\angle(\tilde{\mathbf{h}}_j, \hat{\mathbf{h}}_j)) \right] < 2^{-\left(\frac{B}{M(N-1)}\right)}. \quad (12)$$

Note that (12) follows for  $M=1$ , since  $\tilde{\mathbf{h}}_j$  and  $\hat{\mathbf{h}}_j$  are vectors of size  $N \times 1$ . When  $M > 1$ , the expression can be rewritten as

$$\mathbb{E} \left[ \sin^2(\angle(\tilde{\mathbf{H}}_{jj}, \hat{\mathbf{H}}_{jj})) \right] < 2^{-\left(\frac{B}{M(N-1)}\right)}, \quad \forall M > 1. \quad (13)$$

It is to note in (13) that we are concerned with the angle between the normalized and the estimated channel vector components and not with the angle between two matrices. Thus the expectation of the quantization error is upper bounded by  $2^{-\left(\frac{B}{M(N-1)}\right)}$ .

#### IV. RATE REDUCTION FOR ZEROFORCING BEAMFORMING WITH FRF IN MU-MIMO WLANS

The ZF precoding vector when CSI is perfectly known to the  $j$ th AP is given by

$$\mathbf{v}_j^{zf} = \left( \frac{\prod_{\mathbf{H}_{ij}}^{\perp} \mathbf{H}_{jj}}{\left\| \prod_{\mathbf{H}_{ij}}^{\perp} \mathbf{H}_{jj} \right\|} \mathbf{D} \right) \quad (14)$$

where  $\prod_{\mathbf{H}_{ij}}^{\perp} = \mathbf{I}_N - \mathbf{H}_{ij}(\mathbf{H}_{ij}^H \mathbf{H}_{ij})^{-1} \mathbf{H}_{ij}^H$  denotes the projection onto the orthogonal complement of the column space of  $\mathbf{H}_{ij}$ .  $\mathbf{I}_N$  represents the identity matrix of size  $N$ .  $\mathbf{D} \in \mathbb{C}^{M \times 1}$  is a unit vector acting as a demultiplexer where  $\mathbf{D}^H \mathbf{D} = 1$ . The rate associated with this transmission is given by

$$R_j^{ZF} = N \mathbb{E} \left[ \log_2 \left( 1 + \frac{\gamma \|\mathbf{H}_{jj}\|^2 \left\| \prod_{\mathbf{H}_{ij}}^{\perp} \mathbf{v}_j^{zf} \right\|^2}{\sigma^2} \right) \right]. \quad (15)$$

However, with a FRF, the precoding vector is calculated in the same way as in (14) but with the quantized channel information  $\tilde{\mathbf{H}}_{jj}$  and  $\hat{\mathbf{H}}_{ij}$ . The rate for ZFB with FRF is given by

$$R_j^{FRF} = N \mathbb{E} \left[ \log_2 \left( 1 + \frac{\gamma \|\mathbf{H}_{jj}\|^2 \left\| \tilde{\mathbf{H}}_{jj}^H \hat{\mathbf{v}}_j \right\|^2}{\sigma^2 + \sum_{i \neq j}^K \gamma \|\mathbf{H}_{ij}\|^2 \left\| \tilde{\mathbf{H}}_{ij}^H \hat{\mathbf{v}}_i \right\|^2} \right) \right]. \quad (16)$$

Although ZF beamforming is used, there is residual interference because the beamformer is based on the quantized CSI. Thus we analyze the interference term i.e.,  $\left\| \tilde{\mathbf{H}}_{ij}^H \hat{\mathbf{v}}_i \right\|^2$  in (16) further.

Considering  $M = 1$ , since RVQ is used, the quantization error  $Z$  is isotropically distributed in  $\mathbb{C}^N$ . Thus from [10],

$$\left\| \tilde{\mathbf{h}}_j^H \hat{\mathbf{v}}_i' \right\|^2 = Z \left| \mathbf{g}^H \hat{\mathbf{v}}_i' \right|^2 \leq \sin^2(\angle(\tilde{\mathbf{h}}_j, \hat{\mathbf{h}}_j)), \quad (17)$$

where  $\mathbf{g} \in \mathbb{C}^{N \times 1}$  and  $\hat{\mathbf{v}}_i' \in \mathbb{C}^{N \times 1}$  are vectors in the  $(N-1)$ -dimensional null space of  $\hat{\mathbf{h}}_j$ . The quantity  $\left| \mathbf{g}^H \hat{\mathbf{v}}_i' \right|^2$  is beta  $(1, N-2)$  distributed and is independent of  $Z$ .

For  $M > 1$ , the expectation of the interference term i.e.,  $\mathbb{E} \left[ \left\| \tilde{\mathbf{H}}_{ij}^H \hat{\mathbf{v}}_i \right\|^2 \right]$  is the product of the expectation of the quantization error and the expectation of beta  $(1, N-2)$  random variables, which is equal to  $\frac{1}{N-1}$ . Thus from (13) and (17)

$$\mathbb{E} \left\| \tilde{\mathbf{H}}_{ij}^H \hat{\mathbf{v}}_i \right\|^2 = \left( \frac{1}{(N-1)} \right) 2^{-\left(\frac{B}{M(N-1)}\right)}, \quad \forall M > 1, \quad (18)$$

where  $\hat{\mathbf{v}}_i$  is calculated in the same way as in (14) but with the quantized channel information  $\tilde{\mathbf{H}}_{jj}$  and  $\hat{\mathbf{H}}_{ij}$ .

Since FRF with  $B$  bits per client is used, this incurs a throughput loss relative to perfect CSIT

$$\begin{aligned} \Delta R(P) & \triangleq \frac{1}{N} (R_j^{ZF} - R_j^{FRF}) \\ & = \mathbb{E} \left[ \log_2 \left( \sigma^2 + \gamma \|\mathbf{H}_{jj}\|^2 \left\| \tilde{\mathbf{H}}_{jj}^H \mathbf{v}_j^{zf} \right\|^2 \right) \right] \\ & \quad - \mathbb{E} \left[ \log_2 \left( 1 + \frac{\gamma \|\mathbf{H}_{jj}\|^2 \left\| \tilde{\mathbf{H}}_{jj}^H \hat{\mathbf{v}}_j \right\|^2}{\sigma^2 + \sum_{i \neq j}^K \gamma \|\mathbf{H}_{ij}\|^2 \left\| \tilde{\mathbf{H}}_{ij}^H \hat{\mathbf{v}}_i \right\|^2} \right) \right] \\ & = \mathbb{E} \left[ \log_2 \left( \sigma^2 + \gamma \|\mathbf{H}_{jj}\|^2 \left\| \tilde{\mathbf{H}}_{jj}^H \mathbf{v}_j^{zf} \right\|^2 \right) \right] \\ & \quad - \mathbb{E} \left[ \log_2 \left( \sigma^2 + \sum_{i \neq j}^K \gamma \|\mathbf{H}_{ij}\|^2 \left\| \tilde{\mathbf{H}}_{ij}^H \hat{\mathbf{v}}_i \right\|^2 + \right) \right] \\ & \quad + \mathbb{E} \left[ \log_2 \left( \sigma^2 + \sum_{i \neq j}^K \gamma \|\mathbf{H}_{ij}\|^2 \left\| \tilde{\mathbf{H}}_{ij}^H \hat{\mathbf{v}}_i \right\|^2 \right) \right] \\ & \leq^a \mathbb{E} \left[ \log_2 \left( \sigma^2 + \gamma \|\mathbf{H}_{jj}\|^2 \left\| \tilde{\mathbf{H}}_{jj}^H \mathbf{v}_j^{zf} \right\|^2 \right) \right] \\ & \quad - \mathbb{E} \left[ \log_2 \left( \sigma^2 + \gamma \|\mathbf{H}_{jj}\|^2 \left\| \tilde{\mathbf{H}}_{jj}^H \hat{\mathbf{v}}_j \right\|^2 \right) \right] \\ & \quad + \mathbb{E} \left[ \log_2 \left( \sigma^2 + \sum_{i \neq j}^K \gamma \|\mathbf{H}_{ij}\|^2 \left\| \tilde{\mathbf{H}}_{ij}^H \hat{\mathbf{v}}_i \right\|^2 \right) \right] \\ & =^b \mathbb{E} \left[ \log_2 \left( \sigma^2 + \sum_{i \neq j}^K \gamma \|\mathbf{H}_{ij}\|^2 \left\| \tilde{\mathbf{H}}_{ij}^H \hat{\mathbf{v}}_i \right\|^2 \right) \right]. \end{aligned} \quad (19)$$

The inequality  $a$  follows because  $\sum_{i \neq j}^K \gamma \|\mathbf{H}_{ij}\|^2 \left\| \tilde{\mathbf{H}}_{ij}^H \hat{\mathbf{v}}_i \right\|^2 \geq 0$  and  $\log(\cdot)$  is monotonically increasing function whereas the equality  $b$  follows because  $\mathbb{E} \left[ \log_2 \left( \sigma^2 + \gamma \|\mathbf{H}_{jj}\|^2 \left\| \tilde{\mathbf{H}}_{jj}^H \mathbf{v}_j^{zf} \right\|^2 \right) \right] = \mathbb{E} \left[ \log_2 \left( \sigma^2 + \gamma \|\mathbf{H}_{jj}\|^2 \left\| \tilde{\mathbf{H}}_{jj}^H \hat{\mathbf{v}}_j \right\|^2 \right) \right]$ . Note that  $\mathbf{v}_j^{zf}$  and  $\hat{\mathbf{v}}_j$  are isotropically distributed unit vectors independent of  $\tilde{\mathbf{H}}_{jj}^H$ . Applying Jensen's inequality to the upper bound in  $b$

and exploiting the independence of the channel norm (which satisfies  $\mathbb{E} \left[ \left\| \tilde{\mathbf{H}}_{ij}^H \right\|^2 \right] = N$ ) and the channel direction, we get

$$\begin{aligned} \Delta R(P) &\leq \log_2 \left( \sigma^2 + \gamma (N-1) \mathbb{E} \left[ \left\| \mathbf{H}_{ij} \right\|^2 \right] \mathbb{E} \left[ \left\| \tilde{\mathbf{H}}_{ij}^H \hat{\mathbf{v}}_i \right\|^2 \right] \right) \\ &= \log_2 \left( \sigma^2 + P(N-1) \mathbb{E} \left[ \left\| \tilde{\mathbf{H}}_{ij}^H \hat{\mathbf{v}}_i \right\|^2 \right] \right). \end{aligned} \quad (20)$$

Thus, from (18) and (20) we get

$$\Delta R(P) \leq \log_2 \left( \sigma^2 + P 2^{-\frac{B}{M(N-1)}} \right), \forall M > 1. \quad (21)$$

## V. NUMERICAL ANALYSIS

### A. Error Bound Analysis

Fig.2a is plotted according to the analytical expression (13) which shows that, for an arbitrary fixed feedback bits  $B = 24$  and with an increasing number of antennas at the clients, the error bound is increased. This is an expected result because  $B$  is constant and, whenever  $M$  increases, the limited  $B$  bits have to quantize the increased channel realizations with the dimensionality of  $M$ . This gives rise to the error bound. Also, with an increasing number of antennas at the APs, as for example  $N = 4, 6$  and  $8$ , we see that the error bound is increased. Putting this another way, with increment in  $M$ , the number of feedback bits per antenna i.e.,  $\lambda = \frac{B}{M}$  is decreased. Fig.2b shows that, with fixed  $B$ , the error bound is increased with decreasing  $\lambda$ . In both of these plots we consider  $N \geq M$ .

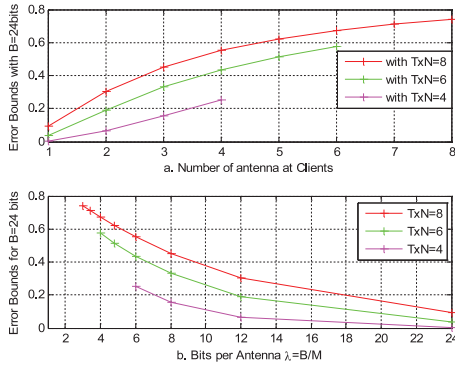


Fig. 2. Error Bounds with: a. number of antennas at clients  $M$  and b. Feedback bits per antenna  $\lambda$ .

### B. Rate with Finite Rate Feedback

We analyze the average rate with FRF at the APs, perfect CSI at the transmitters/APs (CSIT) and without CSI, i.e., noCSIT at the transmitter/APs. Assuming  $M = 1$ ,  $\mathbf{h}_j$ , the ergodic capacity, is given by  $C_{CSIT} = \mathbb{E}[\log_2(1 + P\|\mathbf{h}_j\|^2)]$ . With noCSIT the optimum transmission strategy is to transmit equal power independently to the  $N$  transmit antennas at the APs  $C_{noCSIT} = \mathbb{E}[\log_2(1 + \frac{P}{N}\|\mathbf{h}_{jj}\|^2)]$ . With FRF the average rate achieved assuming RVQ is  $C_{FRF} =$

$$\mathbb{E}[\log_2(1 + P\|\mathbf{h}_j\|^2 \cos^2(\angle \tilde{\mathbf{h}}_j, \hat{\mathbf{h}}_j))] \approx \mathbb{E}[\log_2(1 + P\|\mathbf{h}_j\|^2 (1 - 2^{-\frac{B}{M(N-1)}}))].$$

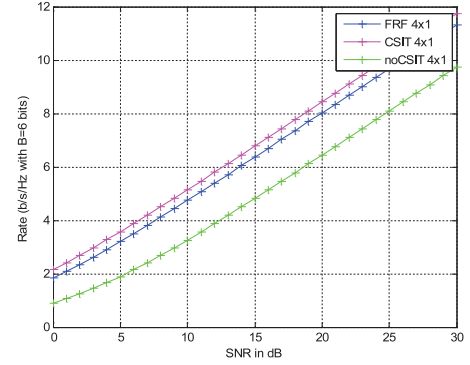


Fig. 3.  $4 \times 1$  MISO capacity with  $B = 6$  bits.

Fig.3 shows the capacity comparison among  $C_{CSIT}$ ,  $C_{FRF}$  and  $C_{noCSIT}$  for  $N = 4$ ,  $M = 1$  and  $B = 6$  bits. The  $C_{FRF}$  lies between  $C_{CSIT}$  and  $C_{noCSIT}$  for a  $4 \times 1$  MISO system with  $B = 6$  bits. Note that  $C_{FRF}$  lies below  $C_{CSIT}$ , which is an expected result as the quantized form of the channels are used for transmissions. The amount of capacity reduction in comparison to  $C_{CSIT}$  is due to the SNR degradation in dB which is given by  $\Delta SNR_{dB} = -10 \log_{10} \left( 1 - 2^{-\frac{B}{M(N-1)}} \right)$ .

For  $N = 4$ ,  $M = 1$  and  $B = 6$  bits,  $\Delta SNR_{dB} = 1.25$  dB. Thus, the capacity in  $C_{FRF}$  is seen to be within about a 1.25 dB gap of  $C_{CSIT}$  in Fig.3. As similar calculation between  $C_{CSIT}$  and  $C_{noCSIT}$  gives a SNR degradation of  $10 \log_{10} N$  dB, which is about 6 dB for a  $4 \times 1$  MISO system with  $B = 6$  bits. Thus we observe three capacity curves at a gap of 1.25 dB and 6 dB from  $C_{CSIT}$  respectively.

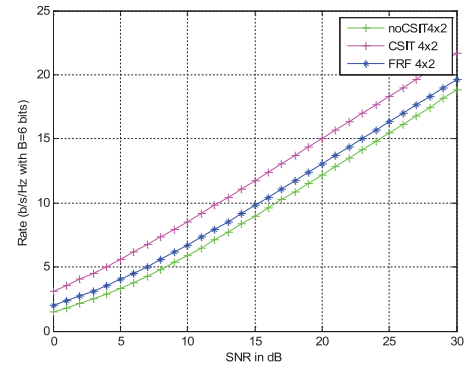


Fig. 4.  $4 \times 2$  MIMO capacity with  $B = 6$  bits.

In Fig.4, we compare the capacity among  $C_{CSIT}$ ,  $C_{FRF}$  and  $C_{noCSIT}$  for  $N = 4$ ,  $M = 2$  and  $B = 6$  bits. We observe that  $C_{FRF}$  lies below  $C_{CSIT}$ . The reason for capacity degradation is due to the use of quantized CSI for transmission.

It is worthwhile to compare Fig.3 and Fig.4 and note that the  $C_{FRF}$  reduction with respect to  $C_{CSIT}$  is greater in a

$4 \times 2$  MIMO system than a  $4 \times 1$  MISO system, as we can see a larger gap in the former. This is because, with increasing antennas at the clients  $M$ , feedback bits per antenna  $\lambda = \frac{B}{M}$  decreases. Also, we know from the error bound analysis and Fig.2 in Section V.A that, with decreasing  $\lambda$ , the error bound is increased. Now, the error bound versus the capacity in Fig.5 shows that, with an increase in error bound,  $C_{FRF}$  decreases. Thus,  $C_{FRF}$  lies below  $C_{CSIT}$  for increasing  $M$ , as shown in Fig.4. The amount of  $C_{FRF}$  reduction is given by the SNR

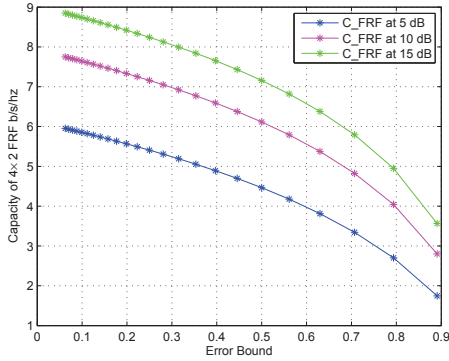


Fig. 5.  $4 \times 2$  MIMO capacity with error bound.

degradation,  $\Delta SNR_{dB}$ . For  $N = 4$ ,  $M = 2$  and  $B = 6$  bits,  $\Delta SNR_{dB} = 3$  dB. Thus,  $C_{FRF}$  performs within about 3 dB of  $C_{CSIT}$  as shown in Fig.4.

### C. Average Rate Reduction for Zeroforcing Beamforming due to FRF

The analytical expression in (21) gives the upper bound of the throughput loss incurred by FRF with respect to CSIT, i.e.,  $\Delta R = C_{CSIT} - C_{FRF}$ . In MU-MIMO with  $B = 6$  bits,  $N = 4$  and 3 clients with  $M = 1, 2$  and 4 receiving antennas, the throughput loss for  $C_{FRF}$  in comparison to  $C_{CSIT}$  is plotted. We observe that, with increase in  $M$ , the throughput loss  $\Delta R$  for  $C_{FRF}$  also increases. This is an expected result because, with increasing  $M$ ,  $\lambda$  decreases, and as a result the error bound increases. With increasing error bound  $C_{FRF}$  decreases. Thus the throughput loss,  $\Delta R$ , increases with increasing  $M$  as shown in Fig.6. Additionally, from (16) and (21),  $R_j^{FRF}$  consists of  $\Delta R(P)$  in the denominator. This term decreases  $R_j^{FRF}$  with increasing SNR, which as a result maintains a constant gap with  $C_{CSIT}$  with increasing SNR.

## VI. CONCLUSION

This paper quantifies both the quantization error bound and the average rate reduction in a MU-MIMO WLAN settings, where the feedback bandwidth  $T_{fb}$ , the number of feedback bits  $B$ , the number of antennas at the APs  $N$  are fixed and the number of antennas at clients  $M$  is variable. We derive a closed form expression for both the quantization error bound and the average rate reduction with respect to perfect CSI. We found that with increasing  $M$  both the quantization error bound and the average rate reduction with respect to perfect CSI increase.

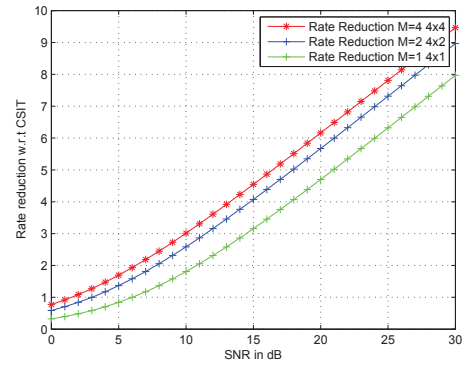


Fig. 6. Average rate reduction due to Finite Rate Feedback when  $B = 6$  bits.

## REFERENCES

- [1] M. H. Costa, "Writing on dirty paper (corresp.)," *Information Theory, IEEE Transactions on*, vol. 29, no. 3, pp. 439–441, 1983.
- [2] U. Erez and S. ten Brink, "A close-to-capacity dirty paper coding scheme," *Information Theory, IEEE Transactions on*, vol. 51, no. 10, pp. 3417–3432, 2005.
- [3] F. Boccardi, F. Tosato, and G. Caire, "Precoding schemes for the mimo-gbc," in *Communications, 2006 International Zurich Seminar on*. IEEE, 2006, pp. 10–13.
- [4] S. Sanjeeb, F. Gengfa, D. Eryk, and H. X., "Addressing hidden terminals in wlans with zeroforcing coordinated beamforming," in *Communications and Information Technologies (ISCIT), 2014 14th International Symposium on*. IEEE, 2014, pp. 249–253.
- [5] S. Sanjeeb, F. Gengfa, D. Eryk, and H. Xiaojing, "Zeroforcing precoding based mac design to address hidden terminals in mu-mimo wlans," in *The 22nd International Conference on Telecommunications (ICT 2015)*, ser. 22, IEEE. Sydney, Australia: IEEE, 27–29 April 2015.
- [6] A. Narula, M. J. Lopez, M. D. Trott, and G. W. Wornell, "Efficient use of side information in multiple-antenna data transmission over fading channels," *Selected Areas in Communications, IEEE Journal on*, vol. 16, no. 8, pp. 1423–1436, 1998.
- [7] D. J. Love, R. W. Heath, and T. Strohmer, "Grassmannian beamforming for multiple-input multiple-output wireless systems," *Information Theory, IEEE Transactions on*, vol. 49, no. 10, pp. 2735–2747, 2003.
- [8] K. K. Mukkavilli, A. Sabharwal, E. Erkip, and B. Aazhang, "On beamforming with finite rate feedback in multiple-antenna systems," *Information Theory, IEEE Transactions on*, vol. 49, no. 10, pp. 2562–2579, 2003.
- [9] P. Ding, D. J. Love, and M. D. Zoltowski, "On the sum rate of channel subspace feedback for multi-antenna broadcast channels," in *Global Telecommunications Conference, 2005. GLOBECOM'05. IEEE*, vol. 5, IEEE, 2005, pp. 5–pp.
- [10] N. Jindal, "Mimo broadcast channels with finite-rate feedback," *Information Theory, IEEE Transactions on*, vol. 52, no. 11, pp. 5045–5060, 2006.
- [11] S. Wiroonsak and H. Michael, "Asymptotic capacity of beamforming with limited feedback," in *IEEE International Symposium on Information Theory*, 2004.
- [12] S. Wiroonsak and H. M. L., "Capacity of beamforming with limited training and feedback," in *Information Theory, 2006 IEEE International Symposium on*. IEEE, 2006, pp. 376–380.
- [13] C. K. Au-Yeung and D. J. Love, "On the performance of random vector quantization limited feedback beamforming in a miso system," *Wireless Communications, IEEE Transactions on*, vol. 6, no. 2, pp. 458–462, 2007.
- [14] A. K. Gupta and S. Nadarajah, *Handbook of beta distribution and its applications*. CRC Press, 2004.
- [15] P. J. Davis, "Leonhard euler's integral: A historical profile of the gamma function: In memoriam: Milton abramowitz," *American Mathematical Monthly*, pp. 849–869, 1959.
- [16] D. Kershaw, "Some extensions of w. gautschi's inequalities for the gamma function," *Mathematics of Computation*, pp. 607–611, 1983.